Cancer Chemother Pharmacol (2010) 66:21–29
DOI 10.1007/s00280-009-1129-z

ORIGINAL ARTICLE

Dihydroartemisinin improves the efficiency of chemotherapeutics in lung carcinomas in vivo and inhibits murine Lewis lung carcinoma cell line growth in vitro

Hui-Jun Zhou · Jia-Li Zhang · Ao Li · Zeng Wang · Xiao-E Lou

Received: 22 June 2009 / Accepted: 2 September 2009 / Published online: 16 September 2009

Abstract
Purpose Dihydroartemisinin (DHA), a semi-synthetic derivative of artemisinin, has exhibited the strongest anti-malarial activity among the derivatives of artemisinin. There is growing evidence that DHA has some impact against tumors. Our purpose was to evaluate in vitro anti-tumoral properties of DHA in the murine Lewis lung carcinoma (LLC) cell line. At the same time, we observed the therapeutic effect of DHA combined with cyclophosphamide (CTX) in the LLC and combined with cisplatin (CDDP) in the human non-small cell lung cancer A549 xenotransplanted carcinoma in vivo.
Methods Cytotoxicity was measured by 3-(4,5-dimethylthiazol-2-yl)-2,5-diphenyltetrazolium bromide method, apoptosis was measured by AO/EB double staining and flow cytometry. The expression of vascular endothelial growth factor (VEGF) receptor KDR/flk-1 was analyzed by western blotting and RT-PCR. In vivo activity of DHA combined with CTX or CDDP was assayed through tumor growth and metastasis.
Results Dihydroartemisinin exhibited high anti-cancer activity in LLC cell line. DHA also induced apoptosis of LLC cells and influenced the expression of VEGF receptor KDR/flk-1. Furthermore, in both tumor xenografts, a greater degree of growth inhibition was achieved when DHA and chemotherapeutics were used in combination. The affection by DHA combined CTX on LLC tumor metastasis was significant.
Conclusions Dihydroartemisinin is a potent compound against LLC cell line in vitro. In vivo, the combination strategy of DHA and chemotherapeutics holds promise for the treatment of relatively large and rapidly growing lung cancers.

Keywords Dihydroartemisinin · Chemotherapeutics · KDR/flk-1 · Apoptosis · Drug combination

H.-J. Zhou (✉) · J.-L. Zhang · A. Li · Z. Wang · X.-E. Lou
Institute of Pharmacology and Toxicology,
College of Pharmaceutical Sciences, Zhejiang University,
388 Yuhang'tang Road, Hangzhou, Zhejiang 310058,
People's Republic of China
e-mail: zhouhj_zhouhj@yahoo.com

Introduction

Lung cancer is the most common cause of cancer mortality worldwide, with over one million deaths each year [1]. The non-small cell lung cancer (NSCLC) is accounting for up to 80% of total pulmonary malignancies [2]. At present, advanced NSCLC is mainly treated by chemotherapy. Although chemotherapy is an anti-cancer management widely used in the treatment of tumors [3, 4], its use is limited by severe toxic side effects. Indeed, a significant reduction in bone marrow proliferation, total white blood cell (WBC) count or neutrophil count was observed on chemotherapeutic used patients [5–7]. Recently, several approaches were developed to try to overcome these problems, such as dose decrease of single agents and multidrug combinations.

Artemisinin is a sesquiterpene lactone endoperoxide found in the traditional Chinese medicinal plant *Artemisia annua* [8, 9], and its derivatives are very effective to blood schistocidal antimalarials with fewer adverse side effects than any other antimalarial drug. Recently, it was reported that artemisinin analogs also showed antitumor activity in vitro and in vivo [10]. Of all the artemisinin derivatives, dihydroartemisinin (DHA), a semi-synthetic derivative of artemisinin, is more water-soluble and effective

antimalarial than artemisinin [11]. Several studies have shown that DHA can inhibit the vascular endothelial growth factor (VEGF) expression in some tumor cells [12, 13]. VEGF is one of the major regulators in a variety of physiological and pathological angiogeneses [14–16]. Its biological activity is mediated by two receptor tyrosine kinases, VEGFR-1 (Flt-1) and VEGFR-2 (KDR/flk-1). As the major receptor for VEGF, KDR/flk-1 has a weaker affinity for VEGF than Flt-1, but promotes strong tyrosine kinase activity, and most of the signaling from VEGF is transduced through KDR/flk-1 [17–20]. It is the major mediator of the mitogenic, angiogenic, and permeability-enhancing effects of VEGF [21, 22].

However, to our knowledge, both chemotherapeutics and DHA have been well studied concerning their activity against tumor cells, while the effectiveness of a combination treatment between them is not know very well. In this paper, an attempt to find whether DHA can improve the efficiency of chemotherapeutics in NSCLC and its possible mechanism, we observed the therapeutic effect of DHA combined with cyclophosphamide (CTX) in the murine Lewis lung carcinoma (LLC) and combined with cisplatin (CDDP) in the human NSCLC A549 xenotransplanted carcinoma in vivo. Besides, we investigated the anti-proliferation and inducing apoptosis effect of DHA on LLC cells, and assessed the expression of VEGF receptor KDR/flk-1 in LLC cells in vitro. The results demonstrated that the combination treatment was more effective than DHA and chemotherapeutics used alone in reducing tumor growth.

Materials and methods

Materials

Dihydroartemisinin was kindly presented by the Engineer, Huali of Jiaxing Pharmaceutical Co. (Zhejiang, China). CDDP was obtained from Qilu Pharmaceutical General Factory, China. CTX was obtained from Hengrui Pharmaceutical Company (Jiangsu, China). Penicillin, streptomycin, dimethyl sulfoxide (DMSO), 3-(4,5-dimethylthiazol-2-yl)-2,5-diphenyltetrazolium bromide (MTT), ethidium bromide and propidium iodide were purchased from Sigma (St Louis, MO, USA). Polyvinylidene difluoride membranes were supplied by Millipore Co. (Billerica, MA, USA). Mouse anti-KDR/flk-1 and goat anti-actin polyclonal antibody (I-19) and all the secondary antisera were purchased from Santa Cruz Biotechnology (Santa Cruz, CA, USA).

Cell culture

The LLC cells and the human NSCLC cell line A549 cells were obtained from the Shanghai Institute of Biochemistry and Cell Biology, Chinese Academy of Sciences (Shanghai, China) and LLC cells were cultured in Dulbecco's modified Eagle's medium (DMEM) while A549 cells were grown in RPMI1640 standard medium supplemented with 10% fetal calf serum and antibiotics (100 IU ml^{-1} penicillin and 100 μg ml^{-1} streptomycin), in humidified air at 37°C with 5% CO_2. Exponentially growing cells were used throughout the study.

Growth inhibition assay

To evaluate the cytotoxicity of DHA, the MTT assay was performed to determine the cell viability. Briefly, cells were seeded at a density of 4×10^3 cells/well in a 96-well plate. Then, the cells were treated with DHA at various concentrations and with 0.2% DMSO as the solvent control. Each concentration was repeated three times. Plates were incubated in a humidified incubator in 5% CO_2 for 48 h at 37°C; 10 μl of MTT solution (5 mg ml^{-1} MTT in PBS stored at 4°C) was then added, and the resulting solution was incubated for 4 h at 37°C in 5% CO_2. Formazan crystals were dissolved in 100 μl of DMSO. The plates were then analyzed in a 96-well format plate reader at 570 nm.

AO/EB double staining

Apoptosis was assessed by fluorescence microscopy (DMIL, Leica), after staining of the cells with a mixture of acridine orange (100 μg ml^{-1}) and ethidium bromide (100 μg ml^{-1}) in PBS. Loss of nuclear structure or fragmented nuclei was taken as indicative of apoptotic cells.

Flow cytometry assay

To evaluate cell cycle profile, the cells (about 1×10^6 cells), pretreated with DHA for 48 h, were harvested, washed twice with PBS and fixed in ice-cold 70% (v/v) ethanol overnight at 4°C. Prior to analysis, samples were washed again and incubated in PBS (pH 7.4) containing 0.1% (v/v) Triton X-100 and 10 mg ml^{-1} RNase A (Sigma) for 30 min, and then incubated with 100 μg ml^{-1} propidium iodide at 37°C in the dark for 30 min. After filtration to remove cellular debris, the single-cell suspensions were analyzed on a flow cytometer (FACS Calibur; Becton-Dickinson, San Jose, CA, USA). Cell cycle parameters were analyzed using Modfit software (Becton-Dickinson).

RT-PCR analysis

Total RNA was isolated from the LLC cells (1×10^6 cells) using Trizol Reagent (Bio Basic) according to the

manufacturer's instructions. The first-strand cDNA was synthesized by M-MLV reverse transcriptase (MBI Fermentas) in a 20 μl reaction system containing 2 μg total RNA. cDNA was amplified by polymerase chain reaction (PCR) using Taq DNA polymerase (MBI Fermentas). PCR was carried out using a Thermal cycler (Eppendorf, Germany) as follows: 94°C for 5 min; 32 cycles at 94°C for 30 s, 60°C for 30 s, and 72°C for 45 s. The PCR products were separated on 1.5% agarose gel and visualized by an ethidium bromide staining. The expression intensities of optimized bands were quantified with Quantity One software. Amplification of glyceraldehyde-3-phosphate dehydrogenase (GAPDH) was used as an internal control. KDR/flk-1 primers: forward, 5′-GATGGGAACCGGAACCT-3′ and reverse, 5′-AATTCCACAATCACCATGAG-3′ [23]; GAPDH primers: forward, 5′-TGACGGGGTCACCCACACTGTGCCCATCTA-3′ and reverse, 5′-CTAGAAGCATTTGCGGTGGACGATGGAGGG-3′ [24].

Western blot analysis

Cell pellet was suspended in cold RIPA buffer [50 mM Tris–HCl (pH 8.0), 150 mM NaCl, 0.1% SDS, 1% sodium deoxycholate, 1% Triton X-100, 1 mM EDTA, and supplemented with 1 mM PMSF and 10 μg ml^{-1} Leupeptin] and incubated on ice for 30 min. The protein concentration was determined using the bicinchoninic acid assay (Bio-Rad). Then equal amounts of protein were separated by a 12% SDS-PAGE and transferred onto polyvinylidene difluoride membrane. Membranes were blocked with 5% non-fat milk, incubated with the primary antibodies at 4°C overnight in PBS-T. Primary antibodies were mouse anti-KDR/flk-1 and goat anti-actin polyclonal antibody (I-19). Immunoreactivity was visualized with horseradish peroxidase-linked secondary antibodies and chemiluminescence, β-actin levels were analyzed as controls for protein loading.

Evaluation of antitumor activity and experimental metastasis assay in vivo

Animals bearing LLC xenograft tumors were treated DHA with CTX

Female mice of inbred strains C57BL/6 were purchased from the Shanghai Laboratory Animal Center, Chinese Academy of Sciences (Shanghai, China) and used at 5–6 weeks of age. All animals were raised under specific pathogen-free conditions in the Animal Center of Zhejiang University, in accordance with the procedures outlined in the Guide for the Care and Use of Laboratory Animals. LLC cells were injected s.c. (1×10^6 cells per mouse in 0.2 ml saline) in the right axillary region of four C57BL/6 mice. When the subcutaneous tumor reached about 1.5 cm in diameter, the mice were killed and small pieces of tumor tissues approximately 1 mm^3 were implanted into the right axillary region of other new recipient mice. On the day after tumor tissue implantation, C57BL/6 mice were randomly placed into eight experimental groups. Each group was composed of ten mice. The eight experimental groups included mice that were administered with saline (control group), CTX (50 mg kg^{-1} day^{-1}), DHA (50, 100, 200 mg kg^{-1} day^{-1}), CTX + DHA (drug combine used groups). CTX was administrated i.p. on every other day for five consecutive times. The mice were killed 25 days after tumor inoculation for the counting of metastatic nodules. The numbers of lung metastases and nodule formations were determined.

Animals bearing A549 xenograft tumors were treated DHA with CDDP

Female mice of inbred strains BALB/c were also purchased from the Shanghai Laboratory Animal Center, Chinese Academy of Sciences (Shanghai, China) and used at 5–6 weeks of age. All animals were raised under specific pathogen-free conditions in the Animal Center of Zhejiang University. The approach to establish A549 tumor model was the same as LLC tumor model. The BALB/c nude mice were monitored regularly after tumor tissue implantation, and when solid tumor volumes reached 80–100 mm^3, administration of two drugs was initiated. Each group had six mice. The drug scheduling copied from LLC tumor model, except the dose of CDDP. CDDP was administrated i.p. 2 mg kg^{-1}.

The extent of tumor growth was measured every other day using sterile metric calipers. Tumor volume was calculated using the following formula: volume $= 0.5 \times (\text{width})^2 \times (\text{length})$ as previously described [25].

Data analysis

The statistical significance of mean values was determined by unpaired two-tailed Student's t test. Significance of dose–response curve was detected by ANOVA.

Results

The anti-proliferation effect of DHA in LLC cells

DHA treated at concentrations of more than 5 μmol l^{-1} for 48 h inhibited the growth of LLC cells in a dose-dependent manner as shown in MTT assay. DHA at 5, 10, 20, 40, 80 and 160 μmol l^{-1} inhibited the growth of cells by 8.74, 15.05, 29.24, 45.78, 62.37 and 70.53%, respectively.

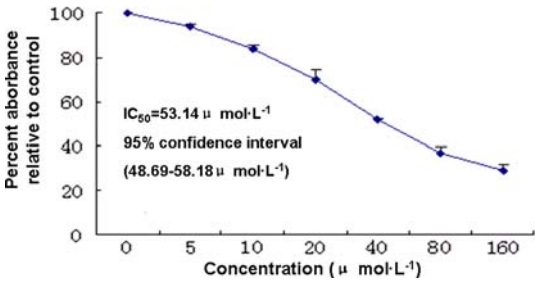

Fig. 1 Effect of DHA on proliferation of LLC cells. LLC cells were seeded into 96-well plates and incubated for 48 h in the presence of DHA with different concentrations. Cell proliferation was detected by MTT assay. The data were from three independent experiments. $\bar{x} \pm s$, $n = 3$

The IC_{50} value of DHA for growth inhibition of LLC cells was 53.14 μmol l^{-1}, and 95% confidence interval was 48.69–58.18 μmol l^{-1} (Fig. 1).

Morphological changes of apoptosis in LLC cells

Acridine orange/ethidium bromide was used to assess changes in nuclear morphology following DHA treatment. The nuclei in normal cells were normal and exhibited diffused staining of the chromatin. However, after exposure to 20, 40, 80 μmol l^{-1} DHA for 48 h, LLC cells underwent typical morphologic changes of apoptosis such as chromatin condensation and shrunken nucleus (Fig. 2). Therefore, these morphological changes suggested the occurrence of apoptosis in LLC cells after treated with DHA.

Percentage of cells undergoing apoptosis in LLC cells

Moreover, the morphological alterations of DNA in DHA-treated LLC cells were supported by flow cytometry analysis. The dose-related increase in DHA-treated LLC cells' apoptosis initially analyzed using flow cytometry. After cells were treated with 20, 40, 80 μmol l^{-1} DHA for 48 h, the rate of apoptosis was detected by PI flow cytometry. The percentage of apoptosis cells increases to 5.54, 9.92, 13.86 (Fig. 3).

Effect of DHA on KDR/flk-1 mRNA expression in LLC cells

To analyze the mechanism underlying the DHA-induced reduction of LLC cells, the level of mRNA for KDR/flk-1 was tested using a RT-PCR assay. LLC cells were exposed to different concentrations of DHA for 48 h, then total RNA was isolated and semi-quantitative RT-PCR performed to measure KDR/flk-1 mRNA. DHA significantly decreased the level of KDR/flk-1 mRNA in LLC

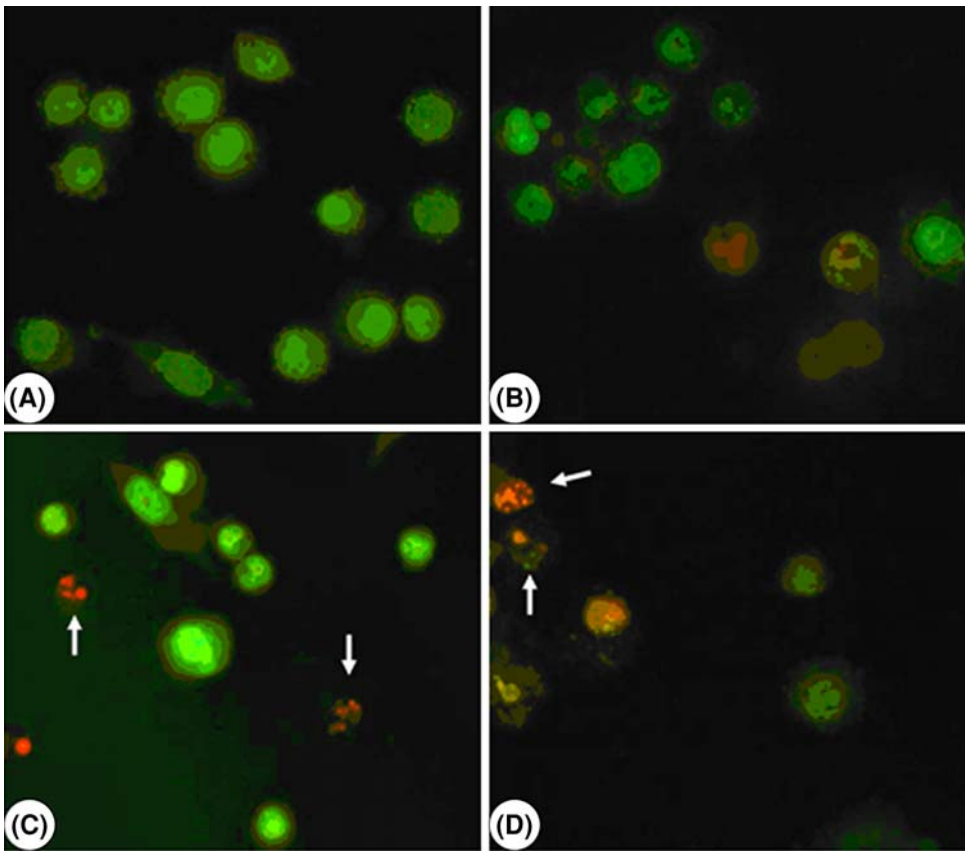

Fig. 2 Fluorescence photomicrographs of LLC cells stained by acridine orange/ethidium bromide (AO/EB) after being treated with DHA. Cells were treated with or without DHA for 48 h. Then the cells were stained by AO/EB and morphology was immediately assessed using fluorescence microscopy (×400). **a** Control cells with intact nuclei structure; **b** DHA 20 μmol l^{-1}; **c**, **d** DHA 40, 80 μmol l^{-1}, respectively, cells shrinkage, chromatin condensation in the nuclei was found (*arrow*)

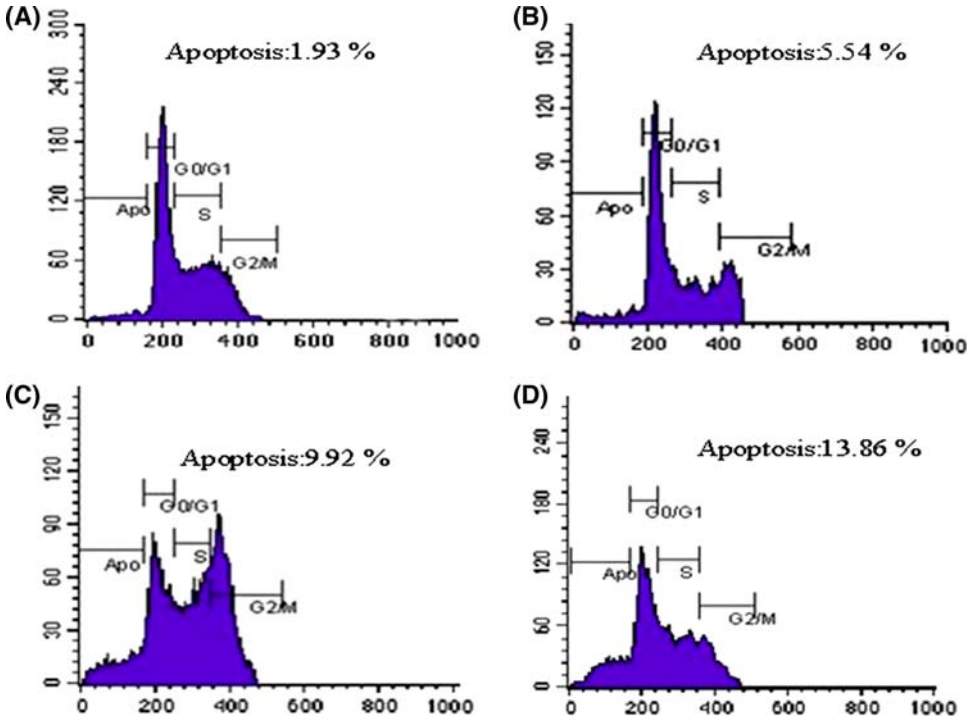

Fig. 3 Flow cytometric analysis of DNA content in LLC cells treated with DMSO or DHA. Cells were incubated with or without DHA for 48 h and analyzed after the addition of PI solution for staining, and cell cycle profiles were determined by flow cytometry. **a** Control cells; **b**, **c**, **d** cells were treated with 20, 40, 80 μmol l^{-1} DHA for 48 h, respectively

cells by 37.53 ± 0.01% (20 μM, $p < 0.05$) and 50.04 ± 0.13% (80 μM, $p < 0.01$), compared to control cells (Fig. 4).

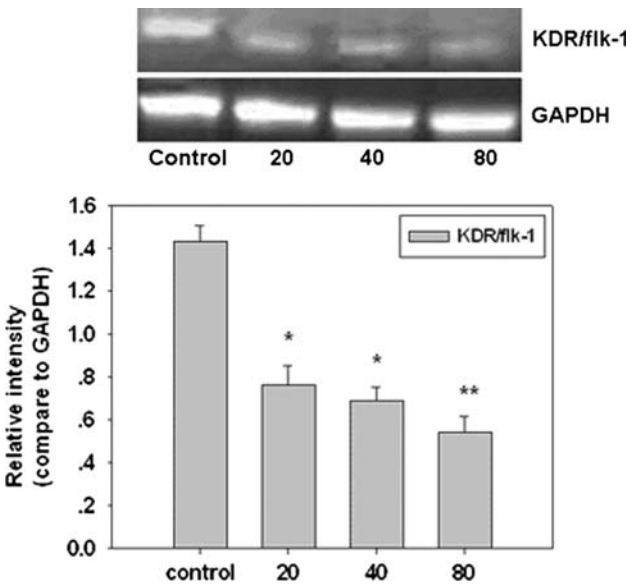

Fig. 4 RT-PCR analysis of the effect of DHA on KDR/flk-1 mRNA levels in LLC cells. LLC cells pretreated with various concentration of DHA for 48 h. The relative expression levels of KDR/flk-1 were expressed as relative intensity compared with GAPDH. Values are mean ± SD of data from three independent experiments. $^{*}p < 0.05$, $^{**}p < 0.01$ versus the control group. $^{\#}p < 0.05$, $^{\#\#}p < 0.01$ versus the control group

Expression of KDR/flk-1 in LLC cells

Western blot was exploited to detect the expression of KDR/flk-1 in LLC cells affected by DHA. LLC cells were treated in vitro with various concentrations of DHA, and were found that increasing concentration of DHA leads to a stepwise reduction in KDR/flk-1 expression. Compared with vehicle control, the levels of KDR/flk-1 in LLC cells were decreased by 33.8 and 12.6% after treated with 40 and 80 μmol l^{-1} DHA for 48 h, respectively ($p < 0.001$) (Fig. 5).

In vivo antitumor effect of DHA in combination with chemotherapeutics

The results in Figs. 6 and 7 show that DHA combined with CTX or CDDP resulted in the significant regression of LLC tumor and A549 tumor compared with either therapy alone. When the test came to the end, in LLC tumor model, the tumor volume of all combination therapy groups was as follows: CTX (50 mg kg^{-1} day^{-1}) + DHA (50, 100, 200 mg kg^{-1} day^{-1}) 729.06 ± 157.07, 326.22 ± 168.69, and 211.37 ± 176.11 mm^3. They were 771.57 ± 329.10, 574.83 ± 269.79, and 472.52 ± 141.79 mm^3 in CDDP (2 mg kg^{-1} day^{-1}) + DHA (50, 100, 200 mg kg^{-1} day^{-1}) groups in A549 tumor model. The tumor volume of combination therapy groups increased less than that of any other treatment groups. After these mice were killed, the solid tumors were peeled off to measure their weights. In both LLC tumor model and A549 tumor model, the tumor

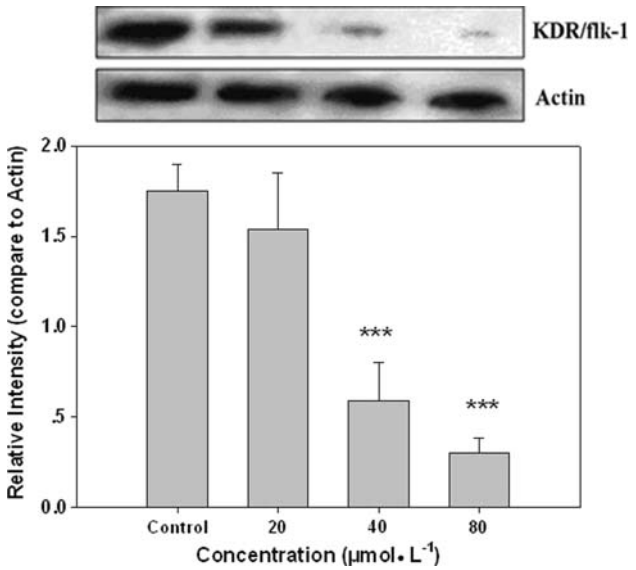

Fig. 5 Western blotting analysis for KDR/flk-1 in LLC cells. Total protein (50 μg) of LLC cells pretreated with various concentration of DHA for 48 h was electrophoresed on 12% SDS-PAGE gel and probed on a PVDF membrane with anti-human KDR/flk-1 antibody. Immune complexes were visualized by enhanced chemiluminescence method using the western blot luminal reagent. Actin levels were analyzed as controls for protein loading. Relative expression levels of KDR/flk-1 were expressed as relative intensity compared with actin. Values are mean ± SD of data from three independent experiments. ***$p < 0.001$ versus the vehicle control group

weights of DHA high-dose combination therapy were significantly less than that of single drug therapy groups ($p < 0.01$, $p < 0.05$). Moreover, the incidence of spontaneous pulmonary metastasis was completely inhibited by the combination of DHA with CTX (Fig. 8). These studies indicate that DHA enhances the ability of CTX and CDDP to inhibit tumor growth and metastasis in murine tumor models. Regarding toxicity, drug-induced body weight loss was not significantly different in any of the therapeutic groups.

Discussion

In our previous studies, we have described the potent antiangiogenic effects of artemisinin derivatives as well as their antitumor effects in vitro [26, 27]. In this study, we have analyzed the anti-proliferative and apoptotic effects of DHA and its regulation of VEGF receptor KDR/flk-1 in LLC cells. From the results of present study, it appeared that DHA may decrease KDR/flk-1 expression, then leading to cell apoptosis. VEGF is a multifunctional cytokine that acts as both a potent inducer of vascular permeability and a specific endothelial cell mitogen [28–31]. The VEGF-induced angiogenesis is mediated mainly by two VEGF receptors, Flt-1 and KDR/flk-1. KDR/flk-1

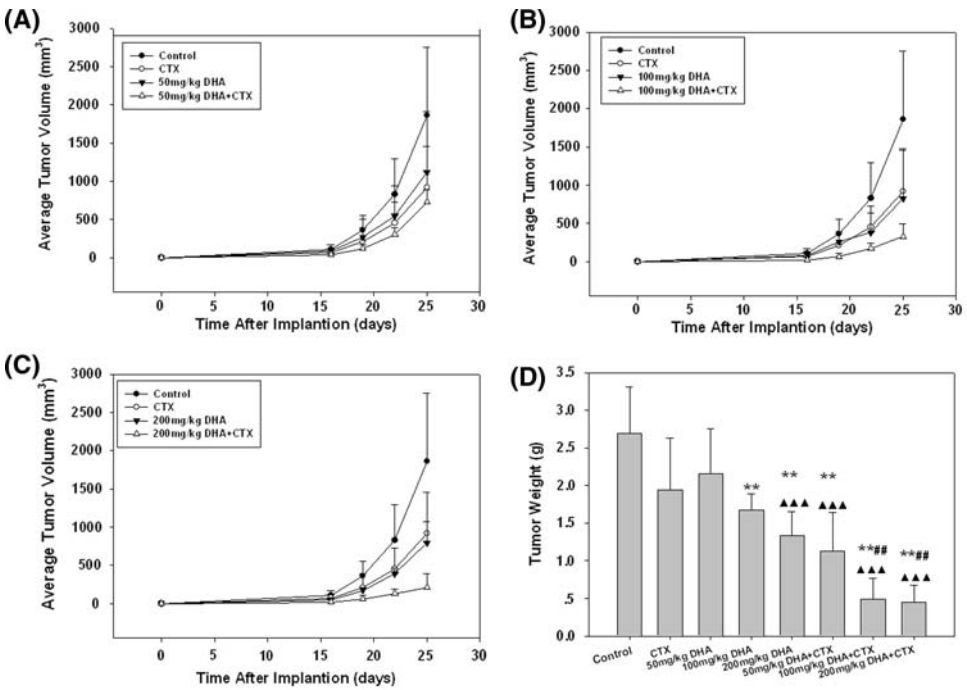

Fig. 6 **a**, **b**, **c** Mean tumor volume in the eight treatment groups of animals. DHA was administrated i.g. daily at 50, 100, 200 mg kg^{-1}, respectively, and CTX was administrated i.p. on every other day for five consecutive times at 50 mg kg^{-1} from day 7. Animals were killed at day 25. The extent of tumor growth was measured every other day using sterile metric calipers. Tumor volume was calculated using the following formula: volume = 0.52 × $(\text{width})^2$ × (length). **d** Effect of DHA combined with or without CTX on LLC xenografted C57BL/6 mice tumor. When animals were killed at day 25, tumors were dissected and weighted. *$p < 0.05$, **$p < 0.01$ versus control. $^{\#}p < 0.05$, $^{\#\#}p < 0.01$ versus DHA. $^{\blacktriangle\blacktriangle}p < 0.01$, $^{\blacktriangle\blacktriangle\blacktriangle}p < 0.001$ versus CTX

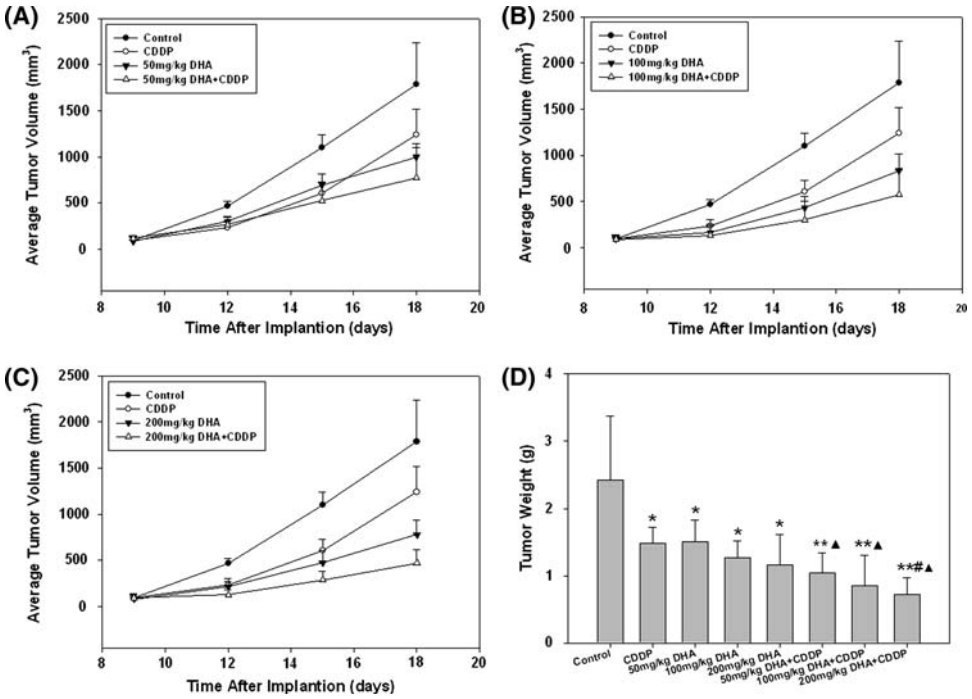

Fig. 7 **a**, **b**, **c** Mean tumor volume in the eight treatment groups of animals. DHA was administrated i.g. daily at 50, 100, 200 mg kg^{-1} from day 6, respectively, and CDDP was administrated i.p. on every other day for four consecutive times at 3 mg kg^{-1} from day 10. Animals were killed at day 18. The extent of tumor growth was measured every other day using sterile metric calipers from day 9. Tumor volume was calculated using the following formula: volume $= 0.52 \times (\text{width})^2 \times (\text{length})$. **d** Effect of DHA combined with or without CDDP on A549 xenografted Balb/c mice tumor. When animals were killed at day 18, tumors were dissected and weighted. $^{*}p < 0.05$, $^{**}p < 0.01$ versus control. $^{\#}p < 0.05$ versus DHA. $^{\blacktriangle}p < 0.05$ versus CDDP

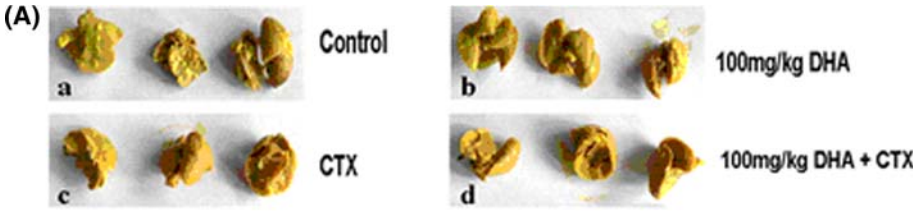

(B)

Groups	Incidence	No.of mratastasis
Control	8/10	10.1
50mg/kg DHA	5/10	1.5
100 mg/kg DHA	4/10	1.1
200mg/kg DHA	2/10	0.9
CTX	4/10	1.3
50 mg/kg DHA+CTX	0/10	0
100 mg/kg DHA+CTX	0/10	0
200 mg/kg DHA+CTX	0/10	0

Fig. 8 **a** External images of the lungs of Lewis lung carcinoma xenografted C57BL/6 mice. Lungs were collected on day 25 after animals were killed. They were immersed into Bouin's liquor first, then dislodged for observation. **b** Pulmonary metastasis affected by DHA combined CTX on LLC xenografted C57BL/6 mice. The numbers of lung metastases and nodule formations were determined

undergoes dimerization and strong ligand-dependent tyrosine phosphorylation in intact cells and results in a mitogenic, chemotactic, and prosurvival signal. Furthermore, KDR/flk-1 (but not Flt-1) activation has been shown to be required for the anti-apoptotic effects of VEGF for human umbilical vein endothelial cells [32]. In the present investigation, we assessed the level of KDR/flk-1 mRNA and protein expression. The experiments suggested that DHA could inhibit the expression of KDR/flk-1 effectively in LLC cells. Based on the above findings, it would seem that KDR/flk-1 expression in LLC is regulated both at the post-transcriptional level and at protein level.

In addition to the antiangiogenic effect of DHA on LLC cells, DHA also found to induce LLC cells apoptosis from our data. This was consistent with previous reports which indicate that the antitumor effect of DHA was ascribed to the rapid induction of apoptosis in cancer cells [33]. Apoptosis includes cell shrinkage and loss of contact with neighboring cells, formation of cytoplasmic vacuoles, plasma and nuclear membrane blebbing, chromatin condensation, and formation of apoptotic bodies [34]. After LLC cells were treated with DHA (20–80 μM) for 48 h, the phase contrast microscopic and fluorescence microscopic observations demonstrated these apoptotic characteristics. Furthermore, the results of flow cytometric analysis of DNA content (Fig. 3) further show that DHA induced 1.93–13.86% increases in the DNA fragments when LLC cells were treated with DHA for 48 h. It has been showed that elevated circulating VEGF level will confer VEGF receptor expression tumor cells with great survival potential and resistance to apoptosis in an autocrine fashion [35]. In our study, we confirmed that DHA downregulated the expression of VEGF receptor KDR/flk-1 in LLC cells, and also induced LLC cells' apoptosis. However, inhibition of VEGF receptor signaling in tumor cells may potentiate the effects of inhibiting anti-apoptotic regulators, or some other survival mechanisms in tumor cells. Overall, the mechanism of artemisinin derivative-induced apoptosis is not understood completely and needs further study.

In the present study, we also investigated the antitumor activity of DHA in vivo. In vivo, DHA combined with CTX resulted in the significant regression of LLC-transplanted tumors compared with either therapy alone (Fig. 6). Moreover, the incidence of spontaneous pulmonary metastasis was completely inhibited by the combination of DHA with CTX (Fig. 8). The data of A549-transplanted tumor model also demonstrated that combination treatment for this tumor model with DHA- plus CDDP-induced greater tumor growth inhibition when compared with treatment in either one of the drugs was used (Fig. 7).

As we know CTX and CDDP are both cytotoxic chemotherapeutics, though chemotherapy has been used in the management of solid cancers for more than half a century and still has been one of the mainstays in the treatment of tumors, most of the chemotherapeutics currently used in chemotherapy are cytotoxic to normal cells, leading to unwanted side effects. The classic toxic side effects of cytotoxic chemotherapy are cardiovascular, gastrointestinal, hematologic, neurological, etc. Therefore, a search for compounds which can reduce the harmful side effects of chemotherapeutics in normal tissues is necessary. In the present study, we used DHA combined with CTX or CDDP. All groups' mice maintained normal activity, without gross signs of cumulative adverse results, such as weight loss, ruffling of fur, behavioral and postural changes. The application of this combination not only had an additive effect on tumor growth inhibition, but also could avoid many of the pronounced side effects in chemotherapy.

Overall, our date has demonstrated that DHA is a potent compound against LLC cell line in vitro and indicates that combination therapy with DHA and chemotherapeutics such as CTX and CDDP is a well protocol with enhanced antitumor activity in vivo. This antitumor activity may be due, in part, to inhibition of angiogenesis via their effects on VEGF receptor and causation of tumor cells' apoptosis. Though further studies on the mechanism of combination therapy are needed, these findings are important for further exploration of potential clinic application of the combined approach. Collectively, these results suggest that DHA is a good candidate for future lung carcinomas treatment strategies. The combination may provide a less toxic, inexpensive and effective cancer chemotherapy.

Acknowledgments This work was supported in part by a grant from the Zhejiang Provincial Science and Technology Program (No. 2008C23067) and by funds for scientific research from Health Bureau of Zhejiang Province (No. 2008W10923), China.

References

1. Parkin DM, Bray F, Ferlay J, Pisani P (2005) Global cancer statistics, 2002. CA Cancer J Clin 55:74–108
2. Zhang F, Zhang T, Gu Z-P et al (2008) Enhancement of radiosensitivity by roscovitine pretreatment in human non-small cell lung cancer A549 cells. J Radiat Res 49:541–548
3. Citron ML (2004) Dose density in adjuvant chemotherapy for breast cancer. Cancer Invest 22:555–568
4. Grinshtein N, Ventresca M, Margl R et al (2009) High-dose chemotherapy augments the efficacy of recombinant adenovirus vaccines and improves the therapeutic outcome. Cancer Gene Ther 16:338–350
5. Morota M, Gomi K, Kozuka T et al (2009) Late toxicity after definitive concurrent chemoradiotherapy for thoracic esophageal carcinoma. Int J Radiat Oncol Biol Phys 75:122–128
6. Suna H-X, Peng X-Y (2008) Protective effect of triterpenoid fractions from the rhizomes of *Astilbe chinensis* on cyclophosphamide-induced toxicity in tumor-bearing mice. J Ethnopharmacol 119:312–317
7. Vincent MD, Dranitsaris G (2009) The price function of toxicity. Lancet Oncol 10:299–303
8. Meshnick SR (2002) Artemisinin: mechanisms of action, resistance and toxicity. Int J Parasitol 32:1655–1660
9. O'Neill PM, Posner GH (2004) A medicinal chemistry perspective on artemisinin and related endoperoxides. J Med Chem 47:2945–2964
10. Efferth T, Dunstan H, Sauerbrey A et al (2001) The anti-malarial artesunate is also active against cancer. Int J Oncol 18:767–773
11. Lai H, Singh NP (2001) Selective toxicity of dihydroartemisinin and holotransferrin toward human breast cancer cells. Life Sci 70:49–56
12. Chen H-H, Zhou H-J, Wang W-Q et al (2004) Antimalarial dihydroartemisinin also inhibits angiogenesis. Cancer Chemother Pharmacol 53:423–432

13. Zhou H-J, Wang W-Q, Wu G-D et al (2007) Artesunate inhibits angiogenesis and downregulates vascular endothelial growth factor expression in chronic myeloid leukemia K562 cells. Vasc Pharmacol 47:131–138
14. Carmeliet P, Ferreira V, Breier G et al (1996) Abnormal blood vessel development and lethality in embryos lacking a single VEGF allele. Nature 380:435–439
15. Folkman J (1995) Angiogenesis in cancer, vascular, rheumatoid and other disease. Nat Med 1:27–31
16. Kvanta A (1995) Expression and regulation of vascular endothelial growth factor in choroidal fibroblasts. Curr Eye Res 14:1015–1020
17. Shibuya M, Ito N, Claesson-Welsh L (1999) Structure and function of VEGF receptor-1 and -2. Curr Top Microbiol Immunol 237:59–83
18. Seetharam L, Gotoh N, Maru Y et al (1995) A unique signal transduction from FLT tyrosine kinase, a receptor for vascular endothelial growth factor VEGF. Oncogene 10:135–147
19. Waltenberger J, Claesson-Welsh L, Siegbahn A et al (1994) Different signal transduction properties of KDR and Flt-1, two receptors for vascular endothelial growth factor. J Biol Chem 269:26988–26995
20. Takahashi T, Yamaguchi S, Chida K, Shibuya M (2001) A single auto-phosphorylation site on KDR/Flk-1 is essential for VEGF-A-dependent activation of PLC-gamma and DNA synthesis in vascular endothelial cells. EMBO J 20:2768–2778
21. Terman BI, Dougher-Vermazen M et al (1992) Identification of the KDR tyrosine kinase as a receptor for vascular endothelial cell growth factor. Biochem Biophys Res Commun 187:1579–1586
22. Millauer B, Wizigmann Voos S, Schnurch H et al (1993) High affinity VEGF binding and developmental expression suggest Flk-1 as a major regulator of vasculogenesis and angiogenesis. Cell 72:835–846
23. Miyamoto N, de Kozak Y, Normand N et al (2008) PIGF-1 and VEGFR-1 pathway regulation of the external epithelial hemato-ocular barrier. A model for retinal edema. Ophthalmic Res 40:203–207
24. Cury PR, de Araujo VC, Canavez F et al (2007) The effect of epidermal growth factor on matrix metalloproteinases and tissue inhibitors of metalloproteinase gene expression in cultured human gingival fibroblasts. Arch Oral Biol 52:585–590
25. Lee EO, Lee HJ, Hwang HS et al (2006) Potent inhibition of Lewis lung cancer growth by heyneanol A from the roots of *Vitis amurensis* through apoptotic and anti-angiogenic activities. Carcinogenesis 27:2059–2069
26. Lee J, Zhou H-J, Wu X-H (2006) Dihydroartemisinin downregulates vascular endothelial growth factor expression and induces apoptosis in chronic myeloid leukemia K562 cells. Cancer Chemother Pharmacol 57:213–220
27. Wu X-H, Zhou H-J, Lee J (2006) Dihydroartemisinin inhibits angiogenesis induced by multiple myeloma RPMI8226 cells under hypoxic conditions via downregulation of vascular endothelial growth factor expression and suppression of vascular endothelial growth factor secretion. Anti-Cancer Drugs 17:839–848
28. Risau W (1997) Mechanisms of angiogenesis. Nature 386:671–674
29. Carmeliet P (2000) Mechanisms of angiogenesis and arteriogenesis. Nature Med 6:389–395
30. Chen HH, Zhou HJ, Wu GD et al (2004) Inhibitory effects of artesunate on angiogenesis and on expressions of vascular endothelial growth factor and VEGF receptor KDR/flk-1. Pharmacology 71:1–9
31. Yancopoulos GD, Davis S, Gale NW et al (2000) Vascular-specific growth factors and blood vessel formation. Nature 407:242–248
32. Gerber H-P, McMurtrey A, Kowalski J et al (1998) VEGF regulates endothelial cell survival by the PI3-kinase/Akt signal transduction pathway. Requirement for Flk-1/KDR activation. J Biol Chem 273:30336–30343
33. Zhou H-J, Wang Z, Li A (2008) Dihydroartemisinin induces apoptosis in human leukemia cells HL60 via downregulation of transferrin receptor expression. Anticancer Drugs 9:247–255
34. Rello S, Stockert JC, Moreno V et al (2005) Morphological criteria to distinguish cell death induced by apoptotic and necrotic treatments. Apoptosis 10:201–208
35. Quinn TP, Soifer SJ, Ramer K et al (2001) Receptor for vascular endothelial growth factor that stimulates endothelial apoptosis. Cancer Res 61:8629–8637